J.Natn.Sci.Foundation Sri Lanka 2011 **39** (1): 35-42

RESEARCH ARTICLE

Thickness dependence of device parameters in solid state dye sensitized solar cells

Jayasundera Bandara[1*] and Mukundan Thelakkat[2]

[1] *Institute of Fundamental Studies, Hantana Road, Kandy.*

[2] *Applied Functional Polymers, Department of Macromolecular Chemistry I, University of Bayreuth, Universitat Strasse 30, 95444 Bayreuth, Germany.*

Submitted: 08 October 2009 ; Accepted: 17 September 2010

Abstract: A solid-state dye-sensitized solar cell (SDSC) was fabricated with a very thin (~ 650 nm) mesoporous TiO_2 electrode and a donor-antenna (D-A) dye by using 2,2′,7,7′-tetrakis-(N,N-di-p-methoxyphenyl-amine) 9,9′-spirobifluorene (Spiro OMeTAD) as hole conductor. A highly transparent thin electrode sensitized with D-A dye showed a short circuit current (I_{sc}) of 4.10 mA/cm^2, an open circuit voltage (V_{oc}) of 782 mV and an efficiency of 1.79 % at an illumination intensity of 100 mW/cm^2 (1 sun, AM 1.5G). $TiCl_4$ treatment of mesoporous TiO_2 layer resulted in I_{sc} of 6.18 mA/cm^2, V_{oc} of 737 mV and an efficiency of 2.12% at the same illumination intensity. This investigation demonstrates the possibility of fabrication of SDSC by way of using a very thin and transparent TiO_2 electrode together with a high molar extinction coefficient D-A dye, and the effect of TiO_2 layer thickness on solid-state solar cell performances is discussed.

Keywords: Donor - antenna dye, sensitization, solid-state dye-sensitized solar cell, TiO_2, transparent electrode.

INTRODUCTION

Dye-sensitized solar cells (DSCs) are an attractive alternative for light-to-electricity conversion applications due to their high efficiency and cost effectiveness (O'Regan & Gratzel, 1991; Tennakone, 2001; Thelakkat, 2002). The liquid electrolyte based DSC is composed of a dye-adsorbed mesoporous TiO_2 electrode, electrolyte containing I^-/I_3^- redox couple and a Pt coated counter electrode. Solid-state dye-sensitized solar cells (SDSC) are also promising due to their large potential to convert solar energy to electrical energy at low cost and their capability to solve the leakage or sealing problems that exist in liquid electrolyte dye-sensitized solar cells (Gratzel, 2003). A typical SDSC consists of several different material layers; an optically transparent compact TiO_2 layer; a dye adsorbed mesoporous nanocrystalline-titanium dioxide n-type semiconductor layer; solid organic or inorganic p-type layer (hole transport layer: HTL) and a gold counter electrode.

In SDSC, photoexcited dyes inject electrons into the conduction band (CB) of the TiO_2 and electron transport to the anode occurs *via* diffusion of electrons through the disordered TiO_2 nanoparticles (van de Lagemaat *et al*., 2006). The diffusion electron transport mechanism plays a decisive role in the mesoporous TiO_2 electrodes because of the absence of an electrical potential gradient in the films (Hagfeldt & Grätzel, 1995; Solbrand *et al*., 1997). The electron transport is limited by grain boundaries of the TiO_2 network and the residence time of electrons in traps. In SDSC fabricated with a mesoporous oxide layer as electron transport media and 2,2′,7,7′ - tetrakis - (N, N-di-p-methoxyphenyl-amine) 9,9′-spirobifluorene (spiro-OMeTAD) as hole conductor, one of the major problems is rapid charge recombination due to the weak electron transport property (Hagfeldt & Grätzel, 1995; Solbrand *et al*., 1997). On one hand, the thickness of the TiO_2 layer has to be the minimum possible for an efficient charge collection by anode. On the other hand, a thicker TiO_2 layer is indispensable to adsorb ample dye so as to absorb greater fraction of incoming sunlight. These two opposing factors, light harvesting and charge collection, lead to an optimal thickness of the TiO_2 layer in SDSCs. A thicker TiO_2 layer results in incomplete pore filling of Spiro-OMeTAD in the mesoporous TiO_2 layer leading to lower efficiency of the cells. i.e. A SDSC fabricated with a semitransparent ~ 2.2 μm thick TiO_2 layer which is sensitized by cis-RuLLV(SCN)2 (L=4,4V-dicarboxylic acid-2,2V-bipyridine, LV=4,4V-dinonyl-2,2V-bipyridine, Z907)

* Corresponding author (jayasundera@yahoo.com)

exhibits an efficiency of ~ 4% at an illumination intensity of 100 mW/cm^2 with Spiro-OMeTAD as hole conductor (Schmidet-Mende *et al.*, 2005; Schmidet-Mende & Gratzel, 2006). The efficiency decreased to 2 % when the TiO_2 film thickness increased to 4 µm. Similar efficiency decreases have been noted for SDSC devices with D-A dye. When ~ 1.3 and 1.7 µm semi-transparent thick TiO_2 layers were sensitized with donor-antenna (D-A) dye such as Ru-TPA-NCS, 3.21 and 1.81% efficiencies have been reported respectively at an illumination intensity of 100 mW/cm^2 with Spiro-OMeTAD as hole conductor (Peng *et al.*, 2004; Snaith *et al.*, 2008). The observed decrease in efficiency with the increase of TiO_2 layer thickness was due to the combined effects of imperfect pore filling of Spiro-OMeTAD in thick mesoporous TiO_2 layer and increased charge recombination. Further, the efficient pore filling of Spiro-OMeTAD has been noticed for thinner TiO_2 layers with the compensation of light absorption. These findings revealed the importance of a thinner transparent TiO_2 layer and a dye with a high absorption coefficient in fabrication of efficient SDSC devices. In this report, fabrication of transparent SDSC devices with thin transparent TiO_2 films, D-A dye such as Ru-TPA-NCS dye having high molar extinction coefficient and Spiro-OMeTAD hole conductor is investigated.

METHODS AND MATERIALS

Titanium(IV)bis(acetoacetonato)-di(isopropanoxylate) (TAA) was purchased from Sigma-Aldrich, USA. Glass substrates (Tec 8, 3mm) covered with fluorine-doped tin oxide (FTO) layer having sheet resistances of 8 Ω per square (Ω/□) were purchased from Hartford Glass Co. Inc., Indiana, USA. The TiO_2 blocking layer (bl-TiO_2) was prepared by spray pyrolysis deposition (SPD) technique (Peng *et al.*, 2004). The TiO_2 precursor TAA (titanium acetylacetonate), diluted with ethanol to a concentration of 0.2 M, was used as the spraying solution and pyrolysis was carried out at 400 °C. After the required number of spraying cycles under optimized conditions, the substrates were annealed at 400 °C for another hour before cooling to room temperature. The substrates were kept in an inert atmosphere for further layer preparation. The nanocrystalline TiO_2 (Dyesol - TiO_2 Paste DSL 18NR-T) and terpinol mixture was deposited on the compact TiO_2 layer by screen-printing. The screen-printed TiO_2 was subsequently sintered by stepwise temperature programming (Karthikeyan *et al*., 2008). The thickness of the TiO_2 layer was varied by using different TiO_2 and terpinol weight ratios.

The TiO_2 layer was coated with dye by leaving them overnight in a 0.5 mM solution of Ru-TPA-NCS dye in Dimethylformamide (DMF). The procedure for the synthesis of the D-A dye has been detailed elsewhere (Karthikeyan *et al*., 2008). After the physisorbed dye molecules were rinsed away by dipping the samples in DMF, the samples were subsequently dried in vacuum at 45 °C for at least 1 h. The hole-transport layer (HTL) was deposited on dye/TiO_2 layer by spin-coating. HTL solution comprises of spiro-OMeTAD (0.16 M), and *tert*-butylpyridine (0.16 mM) dissolved in water-free chlorobenzene. *N*-lithiofluoromethane sulfonamide (Li-salt solution, 30 mM) in cyclohexanone was added as the additive. For each substrate, 70 µL of the hole conductor solution was used for spin-coating. To finish, the Au electrode was deposited by electron beam deposition in a vacuum chamber of BA 510 type from Balzers (Liechtenstein) and the active surface was 0.12 cm^2.

The photovoltaic current–voltage measurements have been carried out by a Keithley 6517 source-measure unit under AM 1.5 G conditions (xenon arc lamp, Air Mass Filters from Oriel). The intensity of light was calibrated with a standard Si-reference cell from the Fraunhofer Institut für Solarenergie (ISE), Freiburg, Germany as 100 mW/cm^2. All efficiency values reported in this work were not corrected with the spectral mismatch factor. The incident photon-to-photocurrent efficiency (IPCE) values were measured using a lock-in amplifier (SR830, Stanford Research Systems) with a current pre–amplifier (SR570, Stanford Research Systems) under shortcircuit conditions after illuminating the devices with monochromatic light from a xenon lamp passing through a monochromator (Spectra-model). UV-Vis spectra were recorded with a Perkin Elmer Lambda 900 spectrometer and the surface and cross-sectional features of TiO_2 layers were examined using LEO 1530 Gemini field emission scanning electron microscope (FE-SEM). TiO_2 films and powders were subjected to Brunauer-Emmet-Teller (BET) experiments by N_2 gas adsorption performed using Micromeritics ASAP 2010 (Accelerated Surface Area and Porosimetry System), USA. Surface areas were obtained from BET examination for both TiO_2 film and powders. X-ray diffraction patterns of the TiO_2 powder and sintered films were examined using Philips X-Pert Multi Purpose X-ray Diffractometer, PW 3040 model with Cu Ka radiation.

RESULTS AND DISCUSSION

The BET measurement of the surface area of the Dyesol-TiO_2 powder which was sintered at 500 µC was 77.6 m^2/g. The BET surface area of the sintered TiO_2 film on FTO glass was not measured, but it was expected to be lower than that of the powdered sample. Figure 1 shows

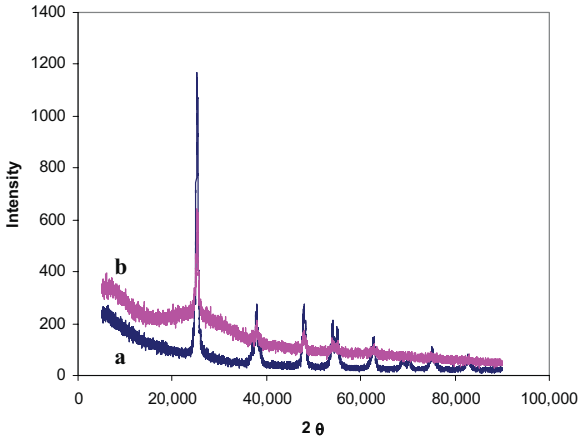

Figure 1: X-ray diffraction patterns of nanocrystalline TiO_2 sintered at 450^o C (a) Dyesol TiO_2 powder and (b) Dyesol-TiO_2 film on FTO – (sample B)

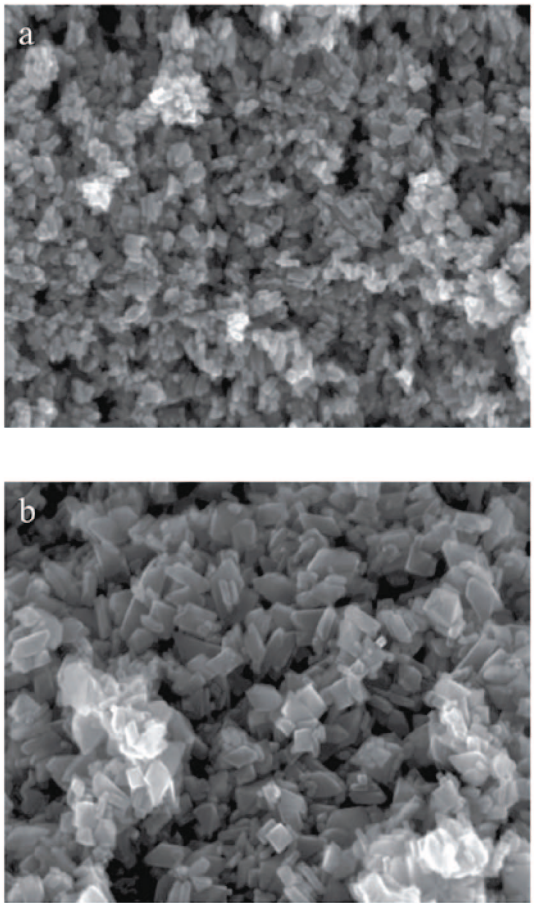

Figure 2: SEM images of (a) Dyesol-TiO_2 film – (sample B), film thickness 0.65 µM and (b) ECN-TiO_2 film, film thickness 0.65 µM after sintering at 450 ^{o}C

the X-ray diffication (XRD) patterns of sintered Dyesol-TiO_2 powder and Dyesol-TiO_2 film on FTO conducting glass. It is evident from the figure that the crystals of both TiO_2 powder and TiO_2 film have pure anatase (101) phase. Taking into account the fast electron transport and high surface area, anatase TiO_2 is the preferred phase for efficient functioning of SDSC (Karthikeyan *et al*., 2007 a, b). To gain better and clear understanding of TiO_2 crystal size, shape and film morphology of the sintered TiO_2 films, which in turn govern the performance in SDSC, Stereo Election Microscope (SEM) examination was carried out for different film thicknesses which were prepared by changing the TiO_2 paste/Terpeniol ratio (0.1: 1, 0.2:1, 0.3:1, 0.4:1, 0.5:1, 0.6:1, 0.7:1, 1:1, 1.5:1 and 2:1 wt/wt). All those TiO_2 films prepared with different dilutions are highly transparent. Figure 2a shows the SEM image of transparent 0.2:1 diluted Dyesol-TiO_2 thin film. For comparison purposes, the SEM image of semi-transparent ECN-TiO_2 thin film is shown in Figure 2b. It is interesting to note that the nanoparticles in both Dyesol-TiO_2 and ECN-TiO_2 films have similar shapes and they are well connected with an optimum pore size. Such a well-connected nanoparticle network is desirable for efficient functioning of SDSC because it will improve the electron percolation of the

Table 1: Variation of film thicknesses of TiO_2 films with the dilution of Terpinol. Film thicknesses were measured with the use of cross-sectional images of different films.

Sample	TiO_2 : Terpinol (wt/wt)	TiO_2 film thickness (µm)
A	0.1 : 1	0.300
B	0.2 : 1	0.650
C	0.3 : 1	0.850
D	0.4 : 1	1.3
E	0.6 : 1	2.4
F	1 : 1	3.1
G	2 : 1	5.8

Table 2: Variations of solar cell performances with the variation of TiO_2 film thicknesess

TiO_2 film thickness (µm)	I_{sc} (mA/cm^2)	V_{oc} (mV)	FF (%)	Efficiency (%)
0.30	3.60	727	40.3	1.05
0.65	4.07	782	54.0	1.72
0.85	6.72	687	38.8	1.70
1.3	6.06	672	39.1	1.59
2.4	3.93	672	41.4	1.12
3.1	2.26	687	30.1	0.47
5.8	1.99	682	29.8	0.41

system. However, the crystal size of Dyesol-TiO_2 is 5-10 nm, whereas ECN-TiO_2 has a large size distribution (10–80 nm). The thickness of the Dyesol-TiO_2 film as a function of dilution of the TiO_2 paste was analyzed by cross-section SEM images of the films. Figures 3a and 3b show the cross-section SEM images of 0.2:1, 0.6:1 and 1.4:1 (wt/wt) diluted Dyesol-TiO_2 films, and the calculated film thicknesses as a function of dilution is given in Table 1. As shown in Table 1, the thickness of the TiO_2 film varied from ~300 nm to ~3.5 μm for 0.1:1 to 1.4:1 (wt/wt) diluted TiO_2 pastes respectively. When the cross-sectional SEM images of the Dyesol-TiO_2 film (Figure 4) were examined at a higher magnification, well dispersed uniform sized nanoparticles that were well connected without forming agglomerates were visible. These well connected nanoparticles facilitate efficient charge transport and collection at the device electrodes.

The molecular structure of the Ru-TPA-NCS D-A dye used in this study is shown in Figure 5a. The extended π-electron delocalization in the bpy ligand enables the D-A dye molecules to have very high molar extinction coefficients ~ 58, 000 $lmol^{-1}$ cm^{-1} at 440 nm and 25, 000 $lmol^{-1}$ cm^{-1} at 540 nm (Karthikeyan *et al*., 2008). The extended separation of electron and holes realized in Ru-TPA-NCS has been shown to retard the recombination process at the TiO_2-dye interface and at the TiO_2-hole conductor interface in solid state solar cells (Handa *et al*., 2007; Boschloo *et al*., 2008). This is of particular interest in SDSCs employing organic hole - transporting materials (HTMs) as it suffers from fast interfacial charge recombination losses relative to liquid electrolyte based devices. Figure 5b shows the absorption spectra of Ru-TPA-NCS adsorbed Dyesol-TiO_2 films as a function of film thickness. For this study, the thickness of TiO_2 film was changed from 300 nm to 2.4 μm. It is clear that thicker samples show better adsorption of the dye compared to thinner ones. It is also evident from Figure 5b that the dye uptake increases linearly with the increase of the TiO_2 film thickness. The quantification amount of adsorbed dye on Dyesol-TiO_2 film cannot be performed accurately owing to difficulty of complete desorbing of the adsorbed Ru-TPA-NCS dye on Dyesol-TiO_2 films.

Since these donor-antenna dyes have extremely high molar extinction coefficients, it is possible to use thinner TiO_2 layers having comparable optical density to that of a thicker TiO_2 film in SDSC application. In order to check this principle, the influence of TiO_2 thickness on SDSC performance was studied using D-A dye Ru-TPA-NCS. I-V characteristics of solar cells fabricated with different TiO_2 film thicknesses (300 nm - 2.4 μm thick TiO_2 films) sensitized with Ru-TPA-NCS dye are shown in Figure 6a and Table 2. Figure 6b shows the plot of variation of short circuit photocurrent density (I_{sc}), open circuit potential (V_{oc}) and efficiency against the film thickness. As shown in Figure 6, the thinnest TiO_2 film (~ 300 nm) showed an I_{sc} of 3.60 $mAcm^{-2}$, a V_{oc} of 727 mV and a fill-factor (FF) of 0.40 resulting in an overall conversion efficiency of ~ 1.05%. Increase in TiO_2 film thickness to ~ 650 nm resulted in increase in I_{sc} (4.2 $mAcm^{-2}$), V_{oc} (782 mV) and FF (0.45 %). As given in Table 2, the optimum I_{sc} (6.72 $mAcm^{-2}$) and efficiency (1.72 %) were noticed when the TiO_2 film thickness was in between 650 – 850 nm and further increase in TiO_2 film thickness resulted in decrease in I_{sc}, V_{oc} and FF. To investigate the variation of solar cell performance with the variation of film thickness of TiO_2, the shunt and series resistances of TiO_2 films were studied as a function of TiO_2 film thicknesses. The dark current-voltage (dark IV) results for different

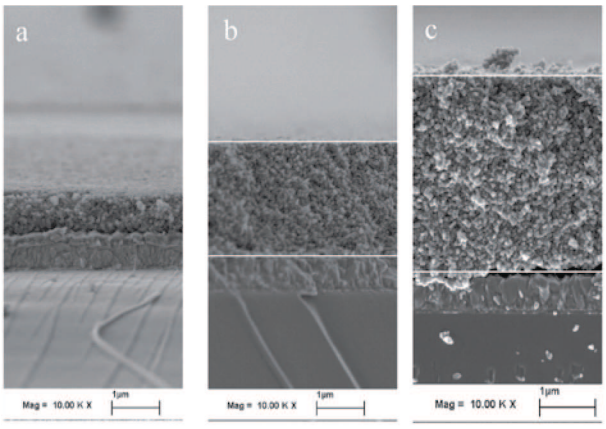

Figure 3: Cross-section view of the Dyesol-TiO_2 film prepared with different dilutions (a) 0.2:1 (sample B - TiO_2:Terpinol wt/wt), (b) 0.6:1 (sample E - TiO_2:Terpinol wt/wt) and (c) 1.4:1 (sample F - TiO_2:Terpinol wt/wt)

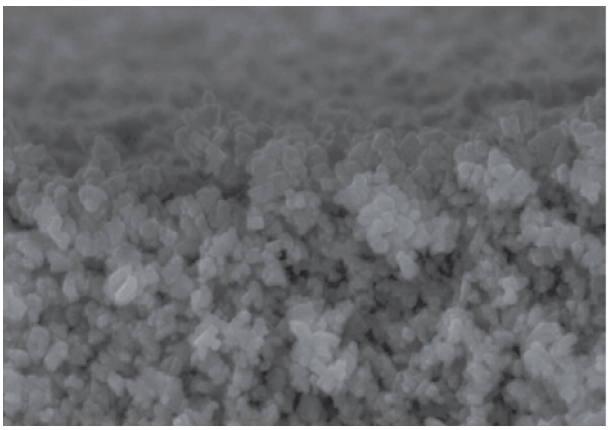

Figure 4: Magnified SEM cross-sectional image of the Dyesol-TiO_2 film 0.2:1 (sample B - TiO_2 : Terpinol wt/wt)

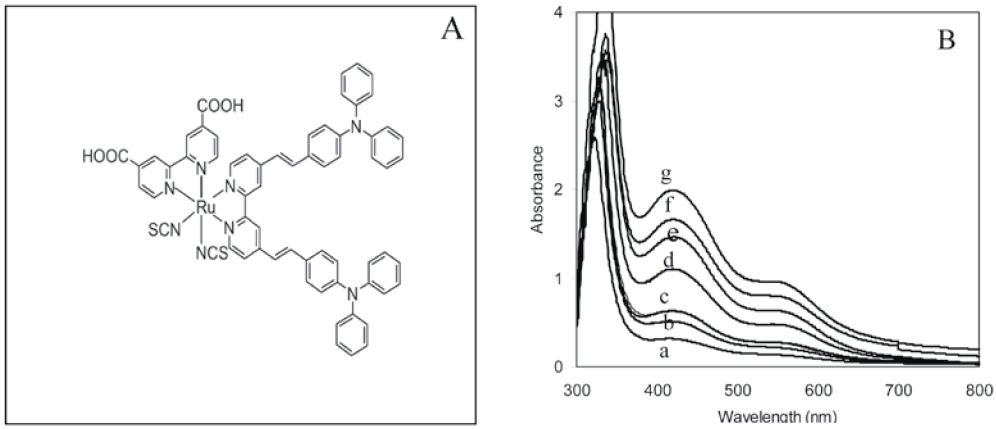

Figure 5: (A) Molecular structure of the Ru-TPA-NCS donor antenna dye, (B) UV-Vis absorption spectra of Ru-TPA-NCS adsorbed Dyesol-TiO_2 film as a function of TiO_2 film thickness (a) 350 nm, (b) 650 nm, (c) 850 nm, (d) 1.3 µm, (e) 2.4 µm, (f) 3.1 µm and (g) 5.8 µm

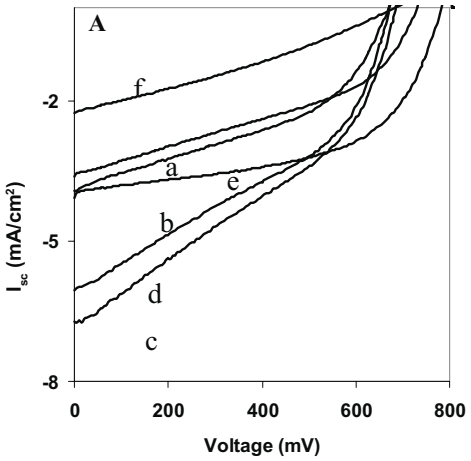

Figure 6(A): Influence of TiO_2 layer thickness on current–voltage characteristics of SDSC prepared with D-A dye, Spiro-OMeTAD with the variation of TiO_2 layer thickness (a) 350 nm, (b) 650 nm, (c) 850 nm, (d) 1.3 µm, (e) 2.4 µm, (f) 3.1 µm and (g) 5.8 µm

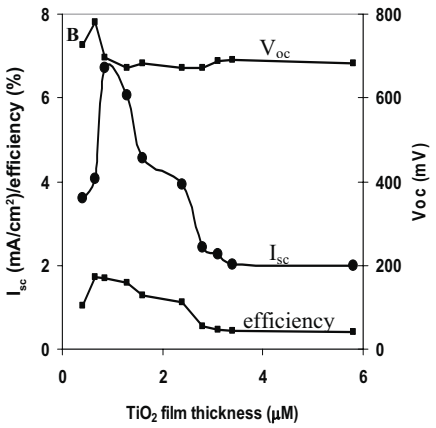

Figure 6(B): Dependence of short circuit current density (mA/cm^2), open circuit potential (mV) and efficiency (%) against TiO_2 film thickness

TiO_2 film thicknesses are shown in Figure 7. It is evident that all the TiO_2 films show good rectification behaviour. Also, it is clearly evident that all the TiO_2 films have high shunt resistance and the shunt resistance is independent of TiO_2 film thickness due to presence of an effective excitone blocking layer (Nazeeruddin *et al*., 2008) which in turn blocks the leakage current from the TiO_2 surface to electrolyte. However, as TiO_2 film thickness increases from 300 nm to 2.4 µm, a dramatic increase in series resistance is noticeable. As given in Table 2, the FF decreases as series resistance increases. Increase in series resistance with the increase of TiO_2 film thickness leads to poor charge collection and hence observed decrease in efficiency as a function of TiO_2 film thickness can be justified (Murayama & Mori, 2006).

From these observations we can conclude that increasing the TiO_2 thickness to an optimum value increases the I_{sc} dramatically leading to higher efficiency compared to thinner cells (300 nm). Higher current for thicker cells is attributed to the higher dye adsorption on thicker TiO_2 films. On the other hand, FF is higher for

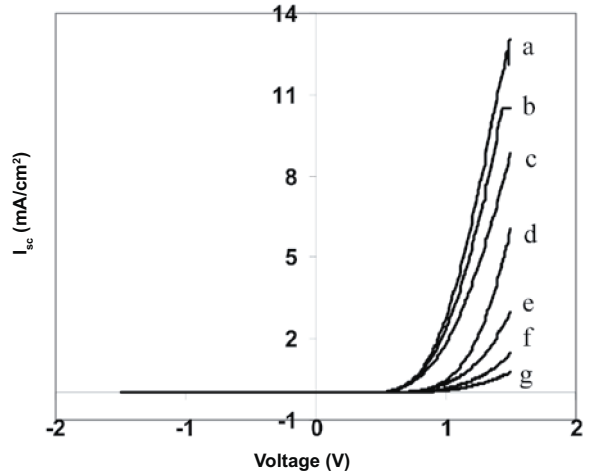

Figure 7: Rectification behaviour of SDSC prepared with D-A dye, Spiro-OMeTAD with the variation of TiO_2 layer thickness (a) 350 nm, (b) 650 nm, (c) 850 nm, (d) 1.3 μm, (e) 2.4 μm, (f) 3.1 μm and (g) 5.8 μm

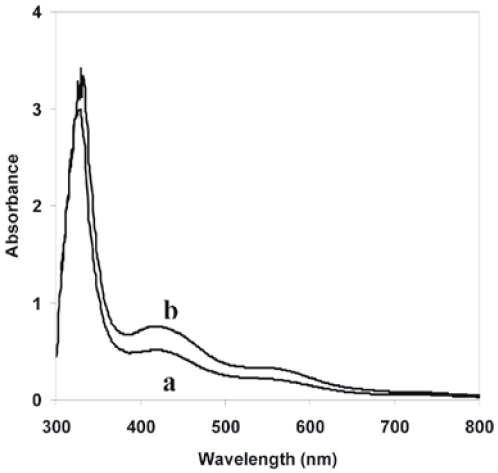

Figure 8: UV-Vis absorption spectra of Ru-TPA-NCS adsorbed 650 nm thick Dyesol-TiO_2 film (sample B- 0.2:1, TiO_2:Terpinol wt/wt) (a) before $TiCl_4$ treatment and (b) after $TiCl_4$ treatment

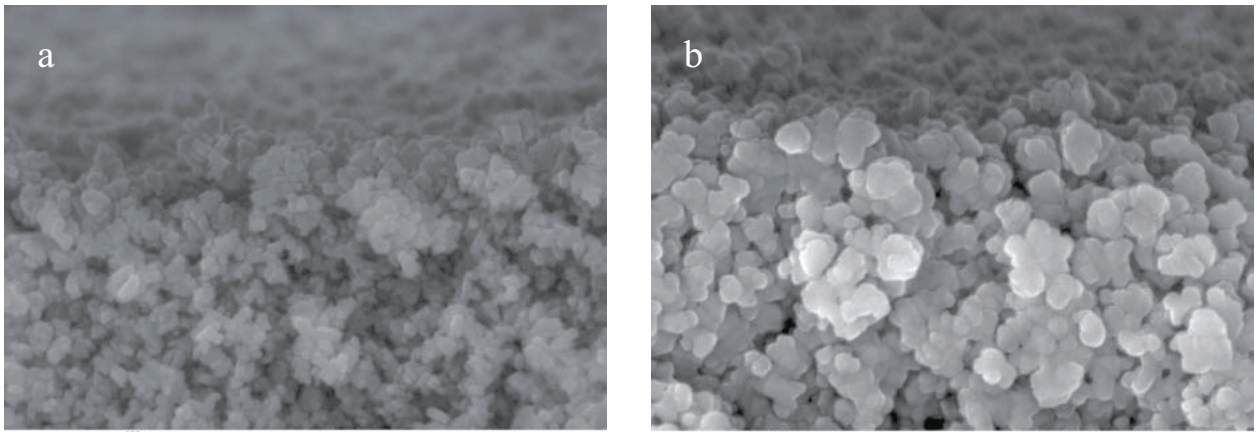

Figure 9: SEM images of 650 nm thick Dyesol-TiO_2 film (sample B - 0.2:1, TiO_2:Terpinol wt/wt) (a) before $TiCl_4$ treatment and (b) after $TiCl_4$ treatment.

thinner cells due to lower series resistance. From this study it is clear that there should be a good balance between the I_{sc} and FF in order to improve the performance of the SDSC. Furthermore, by cross-section SEM images analysis of hole conductor filled thin and thicker TiO_2 films, it was also observed that the pore filling of the hole conductor in thinner TiO_2 films is excellent compared to thicker TiO_2 films. As a result of poor pore filling in thicker TiO_2 films, higher recombination and in turn lower efficiency were expected compared to thinner TiO_2 films.

It is well known that the $TiCl_4$ treatment of the mesoporous TiO_2 layer increases the overall solar cell performance of dye-sensitized solar cells (Sommeling *et al.*, 2006; O'Regan *et al*., 2007). To optimize the solar cell performance further, the optimized solar cell was treated with $TiCl_4$ and sintered at 450 °C. As expected, for $TiCl_4$ treated ~650 nm thick TiO_2 film, I_{sc} and efficiency increased moderately. The observed I_{sc}, V_{oc}, FF and efficiency for $TiCl_4$ treated ~650 nm thick TiO_2 film are 6.18 mAcm^{-2}, 737 mV, 0.44 and 2.1% respectively. Compared to non-treated films, 25% increase in I_{sc} was observed for the $TiCl_4$ treated films while V_{oc} and FF decreased slightly for $TiCl_4$ treated TiO_2 films compared with the optimized SDSC device (650 nm thick TiO_2 film). Comparison of dye-uptake (Figure 8) of both $TiCl_4$ treated and non-treated TiO_2 flms suggest that the

increase in I_{sc} was mainly due to enhanced dye adsorption as a result of increases in the effective surface area available for dye adsorption by increasing the roughness of the TiO_2 particles. Further from SEM images shown in Figure 9a and 9b for $TiCl_4$ treated and non-treated TiO_2 films respectively, the growth of TiO_2 nanocrystallite size after $TiCl_4$ treatment, resulting in enhanced interparticle TiO_2 connection, is clearly evident. Hence, enhanced interparticle connections between TiO_2 particles may result in enhanced charge collection by the anode through percolation of electrons and thereby increase in both I_{sc} and efficiency (Sommeling *et al*., 2006; O'Regan *et al*., 2007).

For the best SDSC device reported to-date, an efficiency of 4 % had been reported with Spiro-OMeTAD as hole conductor and the highest efficiency has been achieved with ~ 2 – 2.5 μm thick TiO_2 film. Therefore, the 2.1% efficiency reported for a thin transparent TiO_2 film (650 nm) in this investigation is remarkable compared to the film thickness of the best SDSC device reported, and could be assigned to high molar extinction coefficient of the D-A dye. The extended π-electron delocalization in the bpy ligand that results enables the D-A dye molecules to have very high molar extinction coefficients-more than twice that of commonly used N-719 dye (Karthikeyan *et al*., 2007). On the other hand, the D-A dye like Ru-TPA-NCS dye is known to minimize charge recombination processes occurring at TiO_2/dye and TiO_2 / hexachloroethane (HC) interfaces by promoting spatial separation of charges due to the presence of electron donating triphenylamine group in the Ru-TPA-NCS. Therefore, it can be said that a high molar extinction coefficient of the donor antenna dye and extended spatial separation of electrons and holes play a significant role in enhancing the solar cell performance. It is known from previous work that the Ru-TPA-NCS dye provides improved performance in solid state solar cells, due partly to the improved wetting of the dye by the spiro-OMETAD hole transporting layer (Karthikeyan *et al*., 2007; Handa *et al*., 2007).

CONCLUSION

An efficient solid-state solar cell was fabricated using 650 nm thick and transparent mesoporous TiO_2 electrodes sensitized with donor antenna dye Ru-TPA-NCS and Spiro-OMeTAD as hole conductor. By $TiCl_4$ treatment of the transparent TiO_2 electrodes, 2.1 % photoconversion efficiency was achieved. A high molar extinction coefficient of the donor antenna dye and extended spatial separation of electrons and holes in the Ru-TPA-NCS are reported to play a significant role in enhancing the solar cell performance due to the improved wetting of the dye by the spiro-OMeTAD hole transporting layer. Thicker transparent TiO_2 electrodes with superior adsorption of Ru-TPA-NCS dye show poor solar cell efficiencies due to poor pore filling of spiro-OMeTAD hole conductor in TiO_2 pores. If an efficient pore filling of hole conductor can be achieved in thicker TiO_2 films, an even more efficient SDSC device can be fabricated.

References

1. Boschloo G., Marinado T., Nonomura K., Edvinsson T., Agrios A.G., Hagberg D.P., Sun L., Quintana M., Karthikeyan C.S., Thelakkat M. & Hagfeldt A. (2008). A comparative study of a polyene-diphenylaniline dye and $Ru(dcbpy)_2(NCS)_2$ in electrolyte-based and solid-state dye-sensitized solar cells. *Thin Solid Films* **516**(20): 7214-7217.
2. Gratzel M. (2003). Dye-sensitized solar cells. *Journal of Photochemistry and Photobiology C: Photochemistry Review* **4** (2):145-153.
3. Hagfeldt A. & Grätzel M. (1995). Light-induced redox reactions in nanocrystalline systems. *Chemical Review* **95**(1): 49-68.
4. Handa S., Wietasch H., Thelakkat M., Durrant J.R. & Haque S.A. (2007). Reducing charge recombination losses in solid state dye sensitized solar cells: the use of donor-acceptor sensitizer dyes. *Chemical Communications* **17**: 1725-1727.
5. Karthikeyan C.S. & Thelakkat M. (2008). Key aspects of individual layers in solid-state dye-sensitized solar cells and novel concepts to improve their performance. *Inorganic Chimica Acta* **361**(3): 635-655.
6. Karthikeyan C.S., Peter K., Wietasch H. & Thelakkat M. (2007). Highly efficient solid-state dye-sensitized TiO_2 solar cells *via* control of retardation of recombination using novel donor-antenna dyes. *Solar Energy Material and Solar Cells* **91**(5): 432-439.
7. Karthikeyan C.S., Wietasch H. & Thelakkat M. (2007). Highly efficient solid-state dye-sensitized TiO_2 solar cells using donor-antenna dyes capable of multistep charge-transfer cascades. *Advanced Material* **9**(8): 1091-1095.
8. Kruger J., Plass R., Gratzel M., Cameron P.J. & Peter L.M. (2003). Charge transport and back reaction in solid-state dye-sensitized solar cells; a study using intensity-modulated photovoltage and photocurrent spectroscopy. *Journal of Physical Chemistry B* **107**(31): 7536-7539.
9. Murayama M. & Mori T. (2006). Equivalent circuit analysis of dye-sensitized solar cell by using one-diode model: effect of carboxylic acid treatment of TiO_2 electrode. *Japanese Journal of Applied Physics* **45**(1B): 542-545.
10. O'Regan B.C., Durrant J.R., Sommeling P.M. & Bakker N.J. (2007). Influence of the $TiCl_4$ treatment on nanocrystalline TiO_2 films in dye-sensitized solar cells. 2. charge density, band edge shifts, and quantification of recombination losses at short circuit. *Journal of Physical Chemistry C* **111**(37): 14001-14010.

11. O'Regan B. & Gratzel M. (1991). A low-cost, high-efficiency solar cell based on dye-sensitized colloidal TiO_2 films. *Nature* **353**(6346): 737-740.
12. Peng B., Jungmann G., Jager C., Haarer D., Schmidt H.W. & Thelakkat M. (2004). Systematic investigation of the role of compact TiO_2 layer in solid state dye-sensitized TiO_2 solar cells. *Coordination Chemical Review* **248**(13-14): 1479-1489.
13. Schmidet-Mende L. & Gratzel M. (2006). TiO_2 pore-filling and its effect on the efficiency of solid-state dye-sensitized solar cells. *Thin Solid Films* **500**(1-2): 296-301.
14. Schmidet-Mende L., Zakuruddin S.M. & Gratzel M. (2005). Efficiency improvement in solid-state-dye-sensitized photovoltaics with an amphiphilic Ruthenium-dye. *Applied Physics Letters* **86**(1): 013504(1)-013501(3).
15. Snaith H.J., Karthikeyan C.S., Petrozza A., Teuscher J., Moser J.E., Nazeeruddin M.K., Thelakkat M. & Grätzel M. (2008). High extinction coefficient "antenna" dye in solid-state dye-sensitized solar cells: a photophysical and electronic study. *Journal of Physical Chemistry C* **112**(20): 7562-7566.
16. Solbrand A., Lindström H., Rensmo H., Hagfeldt A., Lindquist S.E. & Sodergren S. (1997). Electron transport in the nanostructured TiO_2 electrolyte system studied with time-resolved photocurrents. *Journal of Physical Chemistry B* **101**(14): 2514-2518.
17. Sommeling P.M., O'Regan B.C., Haswell R.R., Smit H.J.P., Bakker N.J., Smits J.J.T., Kroon J.M. & vanRoosmalen J.A.M. (2006). Influence of a $TiCl_4$ post-treatment on nanocrystalline TiO_2 films in dye-sensitized solar cells. *Journal of Physical Chemistry B* **110**(39): 19191-19197.
18. Thelakkat M., Schmitz C. & Schmidt H.W. (2002). Fully vapor-deposited thin-layer titanium dioxide solar cells. *Advanced Materials* **14**(8): 577-581.
19. Tennakone K., Bandara J., Bandaranayake K.M.P., Kumara G.R.A. & Konno A. (2001). Enhanced efficiency of a dye-sensitized solar cell made from MgO coated nanocrystalline SnO_2. *Japanese Journal of Applied Physics* **40**(7B): L732-734.
20. van de Lagemaat J., Kopodakos N. & Frank A.J. (2006). Effect of nonideal stastics on electron diffusion in sensitized nanocrystalline TiO_2. *Physical Review B* **71**(3): 1-7.